Polymer 83 (2016) 172–181

Contents lists available at ScienceDirect

Polymer

journal homepage: www.elsevier.com/locate/polymer

Visible-light photopolymerization of DGEBA promoted by silsesquioxanes functionalized with cycloaliphatic epoxy groups

Ignacio E. dell'Erba [a], Gustavo F. Arenas [b], Walter F. Schroeder [a, *]

[a] Institute of Materials Science and Technology (INTEMA), University of Mar del Plata – National Research Council (CONICET), Av. Juan B. Justo 4302, 7600 Mar del Plata, Argentina
[b] Laser Laboratory, Department of Physics, University of Mar del Plata – National Research Council (CONICET), Av. Juan B. Justo 4302, 7600 Mar del Plata, Argentina

ARTICLE INFO

Article history:
Received 5 September 2015
Received in revised form
4 December 2015
Accepted 9 December 2015
Available online 15 December 2015

Keywords:
Photoinitiated cationic polymerization
Epoxy networks
Silsesquioxanes

ABSTRACT

Diglycidyl ether of bisphenol A (DGEBA) is among the most popular and widely used epoxy monomers. This monomer is commonly used in thermal network polymerizations with amines, phenols, isocyanates or mercaptans as curing agents. However, the photoinitiated polymerization of DGEBA is very sluggish and hence finds little use in high-speed photocuring applications. In this contribution, we demonstrated that this monomer can undergo very fast visible-light photopolymerization when combined with a silsesquioxane (SSO) functionalized with reactive epoxycyclohexane groups. The SSO was synthesized via alkoxysilane hydrolysis/condensation chemistry, using DGEBA as a solvent. We found that the photopolymerization of DGEBA is markedly accelerated as the amount of SSO in the mixture is increased. The promoter effect on the reactivity of DGEBA was ascribed to a combination of both thermal and copolymerization effects. Using dynamic mechanical analysis, we demonstrated that the resulting hybrid materials present a single-phase network structure, where the SSO species function as highly multifunctional epoxy reactants.

1. Introduction

Photoinitiated cationic ring-opening polymerization of multifunctional epoxy monomers has been the subject of extensive studies during the last two decades, as this technology has found broad use in a variety of commercial applications, such as coatings, adhesives, encapsulation of electronic components, printing inks, and stereolithography [1–4]. The adoption of this technology is driven by several motivating factors [5–7]. First, these polymerizations proceed rapidly, with low energy and without the use of an inert atmosphere, which provides important economic incentives. Second, the process is solvent-free; therefore, the environmental consequences of these polymerizations are minimal. Furthermore, the network polymers that are formed exhibit outstanding thermal, mechanical and chemical properties, low shrinkage, and very high adhesion to a variety of surfaces [8].

Cationic ring-opening photopolymerizations are commonly initiated with the aid of onium salts [9–11]. Diaryliodonium salts in combination with visible light photosensitizers, such as carbazoles, phenothiazines or camphorquinone, provide a convenient method to generate strong Brønsted acids that initiate cationic ring-opening polymerizations by visible light irradiation [12–16]. The photogenerated acids very rapidly protonate the epoxy groups to form oxonium ion intermediates that proceed further to give polymer. It has been well documented that epoxy monomers display a broad range of reactivity in cationic photopolymerization, which is related to their molecular structures [17,18]. The overall rate of photopolymerization of an epoxy monomer depends mainly on the stability of the oxonium ion intermediates. It has been observed that cycloaliphatic epoxides that bear no means of stabilizing the oxonium ion intermediates undergo very rapid polymerization on UV or visible light irradiation [17]. Under the same irradiation conditions, alkyl glycidyl ethers that bear neighboring oxygen atoms in the structure able to stabilize the oxonium intermediates exhibit long induction periods prior to the onset of polymerization, whereas aryl glycidyl ethers polymerize slowly [17]. Therefore, practical applications that require short irradiation periods and high polymerization rate are currently restricted to a relatively few, typically expensive epoxy monomers. The photoinitiated polymerization of other commercially available and less

* Corresponding author.
E-mail address: wschroeder@fi.mdp.edu.ar (W.F. Schroeder).

http://dx.doi.org/10.1016/j.polymer.2015.12.013
0032-3861/

expensive epoxy monomers, such as diglycidyl ether of bisphenol A (DGEBA), is very sluggish and hence finds little use in commercial applications.

In recent years, interest has been directed toward the development of strategies to effectively accelerate the cationic ring-opening photopolymerization of low-cost epoxy monomers that undergo overall slow reaction. One way to accelerate the photopolymerization of these epoxy monomers is simply increasing the reaction temperature. It has long been known that the overall rates of cationic polymerizations are highly sensitive towards variations in the temperature [19–21]. Even a slight increase in temperature results in destabilization of the oxonium ion intermediates, with the consequent increase in the rate of polymerization. It has also been demonstrated that the induction period of alkyl glycidyl ethers can be markedly shortened through the copolymerization of these monomers with more reactive epoxy monomers [17]. Clearly, if the cationic photopolymerization of low-cost epoxy monomers could be markedly accelerated, these monomers might find numerous uses in high-speed photocuring applications.

In this contribution, we synthesized silsesquioxanes (SSOs) functionalized with cycloaliphatic epoxy groups and explored their virtues to promote the cationic ring-opening photopolymerization of DGEBA. SSOs are an important class of hybrid organic-inorganic compounds obtained by the hydrolytic condensation of organotrialkoxysilanes, $RSi(OR')_3$, performed in the presence of an acid or base as catalysts [22]. Depending upon the synthesis conditions, the species present in SSOs may vary from perfect polyhedra of the formula $(RSiO_{1.5})_n$ (where n is an even number ≥ 6) to partially hydrolyzed/condensed species of the generic formula $T_n(OH)_x(OR')_y$, where $T = RSiO_{1.5-m/2n}$ and $m = x + y$. Some representative species of SSOs are depicted in Scheme 1.

The introduction of appropriate functionalities in the organic branch (R) has been used to incorporate SSOs into polymer chains or networks by covalent bonding. A variety of SSO-containing copolymers have been prepared using condensation, ring-opening metathesis and radical copolymerization techniques [23–27]. The inorganic nature and multiple reactive organic functionalities of SSOs make these compounds ideal for their use in the construction of organic-inorganic hybrid nanomaterials. The incorporation of SSOs into polymers often results in interesting improvements in the material properties, such as higher T_g, oxidation resistance, surface hardening, and enhanced mechanical properties [28,29].

In this work, we synthesized a SSO functionalized with cycloaliphatic epoxy groups via alkoxysilane hydrolysis/condensation chemistry, using DGEBA as a solvent. The resulting SSO/DGEBA solution was characterized by size exclusion chromatography, ultraviolet matrix assisted laser desorption-ionization mass spectrometry (UV-MALDI MS), and IR spectroscopy. Then, we evaluated the ability of the SSO species to accelerate the cationic ring-opening photopolymerization of DGEBA. Finally, the thermomechanical properties of the light-cured hybrid epoxy-based networks were analyzed.

2. Experimental Section

2.1. Materials

The epoxy monomers used in this study were diglycidyl ether of bisphenol A (DGEBA, DER 332 Aldrich Chemical Co.) and 3,4-epoxycyclohexylmethyl 3,4-epoxycyclohexanecarboxylate (EEC, Aldrich Chem. Co). The silane containing a cycloaliphatic epoxy group in its organic chain was trimethoxy[2-(7-oxabicyclo[4.1.0] hept-3-yl)ethyl]silane (TOHES, Aldrich Chem. Co., 98%). The structures of these chemicals are shown in Fig. 1 *p*-(octyloxyphenyl) phenyliodonium hexafluoroantimonate (Ph_2ISbF_6) was supplied by Gelest Inc. (Philadelphia, USA). Camphorquinone (CQ), ethyl-4-dimethyl aminobenzoate (EDMAB), formic acid (ACS reagent, 88–91%), and boron trifluoride ethylamine complex ($BF_3 \cdot MEA$) were from Aldrich Chem. Co. Tetrahydrofuran (THF, ACS reagent >99.0%) was purchased from Cicarelli (Santa Fe, Argentina). All the materials were used as received.

2.2. Synthesis of the silsesquioxane (SSO)

The SSO was prepared by hydrolytic condensation of TOHES, following a procedure in three steps previously reported by Williams and co-workers [30]. Firstly, 1.5 g TOHES was dissolved in 1 mL THF, and then formic acid (0.1 N) was added until reaching a H_2O/Si molar ratio equal to 3. The reaction was carried out in an open vessel for 24 h at 50 °C, enabling the continuous evaporation of volatile products. The second step was performed by adding DGEBA as a solvent in an appropriate amount such that 30% of the epoxy groups were contributed by the SSO. The hydrolytic condensation was continued for another 24 h at 70 °C. The third and last step was performed using the following heating schedule: 3 h at 75 °C, 6 h at 105 °C, and 6 h at 140 °C, allowing complete evaporation of volatile products. The solutions remained homogeneous during the three steps.

An SSO sample was also prepared in the absence of DGEBA. This sample (denoted SSO_{neat}) was prepared with the purpose of evaluating its heat capacity (see section 3.3). For this sample, TOHES (1.5 g) was dissolved in 1 mL THF, and then formic acid was added keeping the molar ratio $H_2O/Si = 3$. The reaction was performed in an open vessel, using temperatures lower than those used for the previous SSO in order to avoid the overall gelation: 24 h at 50 °C, 24 h at 70 °C, 3 h at 75 °C, and 2 h at 90 °C. Therefore, the SSO_{neat} was structurally similar but not identical to the SSO prepared using DGEBA as a solvent.

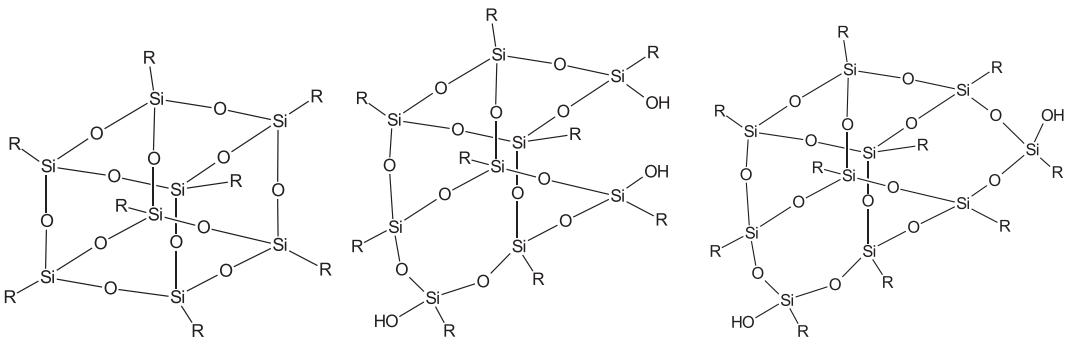

Scheme 1. Schematic drawing of some SSO structures: $R_8Si_8O_{12}$, $R_9Si_9O_{12}(OH)_3$, $R_{10}Si_{10}O_{14}(OH)_2$.

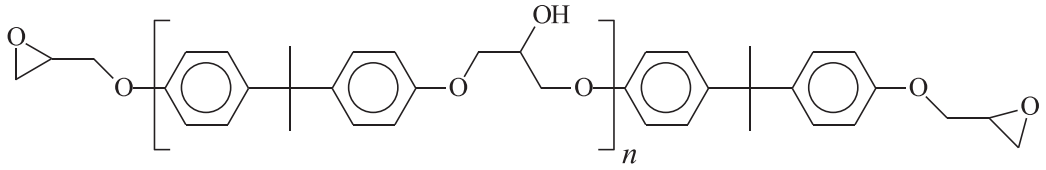

Diglycidyl ether of bisphenol A (DGEBA, $n = 0.03$)

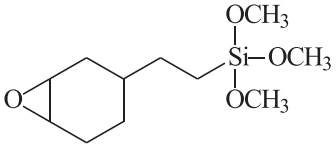

Trimethoxy[2-(7-oxabicyclo[4.1.0]hept-3-yl)ethyl]silane (TOHES)

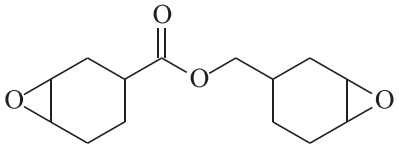

3,4-Epoxycyclohexylmethyl 3,4-epoxycyclohexanecarboxylate (EEC)

Fig. 1. Chemical structure of DGEBA, TOHES and EEC.

2.3. Photopolymerization

After hydrolytic condensation, the SSO/DGEBA solution was diluted with appropriate amounts of DGEBA to prepare samples where the contribution of epoxy groups from the SSO varies between 30% and 10%. For example, the 20:80 SSO/DGEBA designation indicates that 20% of the epoxy groups in the mixture originates from the SSO. The SSO/DGEBA samples were activated for visible light polymerization by the addition of 2 wt% Ph_2ISbF_6 in combination with 1 wt% CQ and 1 wt% EDMAB. The radiation source was a LED unit (VALO, Ultradent; USA) with a wavelength range of 410–530 nm and irradiance equal to 600 mW/cm^2. The intensity of the LED was measured with the chemical actinometer potassium ferrioxalate, which is recommended for the 253–577 nm wavelength range.

2.4. Characterization techniques

Size Exclusion Chromatography (SEC). SEC was performed in a Knauer K-501 device using the following set of columns: Phenogel 5μ M2, Phenogel 5μ 100 Å, Phenogel 5μ 50 Å, and Ultrastyragel 10 Å; and a refractive index detector (Knauer K-2301). THF was used as a carrier at 1 mL/min.

Fourier Transform Infrared Spectroscopy (FTIR). Infrared spectra were recorded with a Nicolet 6700 Thermo Scientific spectrometer at room temperature. Near-infrared (NIR) spectra in transmission mode were acquired over the range of 4000–7000 cm^{-1} from 32 co-added scans at 4 cm^{-1} resolution. The uncured sample was sandwiched between two glass plates separated by a 2-mm rubber spacer ring used to regulate the sample thickness. With the assembly in a vertical position, the radiation source was placed in contact with the glass surface. The specimens were irradiated at regular time intervals and spectra were collected immediately after each exposure interval. The background spectra were collected through an empty mold assembly fitted with only one glass slide to avoid internal reflectance patterns. The conversion of epoxy groups in DGEBA was followed by measuring the height of the absorption band at 4530 cm^{-1} with respect to the height of a reference band at 4620 cm^{-1}. The conversion of epoxy groups in the SSO was evaluated from the decay of the peak at 884 cm^{-1}, using the peak at 1608 cm^{-1} as a reference. Mid-infrared (MIR) spectra were acquired with an attenuated total reflectance (ATR) accessory equipped with a diamond crystal (4 cm^{-1}, 64 scans). Three replicates of each formulation were used in the measurements of conversion.

Temperature evolution during photopolymerization. The evolution of temperature during polymerization was monitored with a *T*-type thermocouple directly plunged into the monomer specimen in the upper half of the sample, where the temperature is more uniform. The thermocouple was connected to a data acquisition system that recorded temperature every 2 s. Studies were conducted on samples of 2 mm thick and 10 mm diameter, identical to those used in the conversion measurements. Three replicates were conducted for each experiment.

Differential Scanning Calorimetry (DSC). Calorimetric measurements were performed using a Shimadzu DSC-50 differential scanning calorimeter under a dry nitrogen atmosphere. The heat capacity at constant pressure (Cp) of the different SSO/DGEBA mixtures was evaluated from DSC curves in dynamic mode [31]. For all the scans, a rate of 10 °C/min was used. Cp was calculated from the following equation,

$$\frac{dH}{dT} = \frac{\left(\frac{dH}{dt}\right)}{\left(\frac{dT}{dt}\right)} = m.Cp \quad (1)$$

where dH/dt is the power input in a dynamic run in DSC, dT/dt is

the heating rate, and *m* is the sample mass. For all the formulations studied in this work, *Cp* was evaluated in the temperature range from 60 °C to 120 °C, where it was found to be nearly constant.

Dynamic Mechanical Analysis (DMA). DMA tests were performed using an Anton Paar, Physica MCR 301 rheometer. All test specimens were photopolymerized under continuous irradiation for 120 s on each side. A set of specimens was also subjected to a thermal postcuring treatment, at 180 °C for 2 h, after photo-irradiation. DMA tests were performed in torsion geometry, using rectangular specimens with dimensions of 30 x 10 × 2 mm^3. Measurements were carried out at 30 °C for the irradiated specimens and as temperature ramps (in the range from 20 °C to 250 °C at a heating rate of 5 °C/min) for the specimens subjected to the additional thermal postcuring treatment. The frequency was kept at 1 Hz and the applied deformation was 0.5%. DMA tests were performed using four specimens for each formulation.

Ultraviolet Matrix Assisted Laser Desorption-Ionization Mass Spectrometry (UV-MALDI MS). Measurements were performed using a Bruker Daltonics Ultraflex II TOF/TOF mass spectrometer (Leipzig, Germany), in the CEQUIBIEM Laboratory (CONICET-Department of Organic Chemistry, University of Buenos Aires, Argentina). Mass spectra were acquired in linear positive and negative ion modes. Several chemicals were attempted as matrices: 9H-pyrido[3,4-b]indole (norharmane), 2,5-dihydroxybenzoic acid (gentisic acid, GA), 3,5-dimethoxy-4-hydroxycinnamic acid (SA), and alpha-cyano-4-hydroxycinnamic acid (CHCA). These chemicals were purchased from Aldrich Chemical Co. External mass calibration was made using β-cyclodextrin (Aldrich Chemical Co) with norharmane as matrix in positive and negative ion mode. The matrix signal was used as an additional standard for calibration in both ionization modes.

Stock solutions of the sample (analyte) were prepared in THF (Aldrich, HPLC grade). Sample solutions were spotted on a MTP 384 polished stainless steel target plate from Bruker Daltonics (Leipzig, Germany). Matrix solutions were prepared by dissolving the chosen matrix compound (1 mg/mL) in acetonitrile/water (1:1, v/v) solution. Water of very low conductivity (Milli Q grade) was used. A sandwich method of sample preparation was used according to Nonami et al. [32], i.e. loading successively 0.5 μL of matrix solution, analyte solution and matrix solution after drying each layer at normal atmosphere and room temperature. Runs were carried out by doping the samples with Na^+. Desorption/ionization was obtained by using a frequency-tripled Nd:YAG laser (355 nm). Experiments were performed using firstly the full range setting for laser firing position in order to select the optimal position for data collection, and secondly fixing the laser firing position in the sample sweet spots. The laser power was adjusted to obtain high signal-to-noise ratio while ensuring minimal fragmentation of the parent ions. Each mass spectrum was generated by averaging 100 lasers pulses per spot.

3. Results and discussion

3.1. Synthesis of epoxy-functionalized silsesquioxanes

The protocol used here followed the strategy developed by Williams and co-workers to synthesize SSOs polyfunctionalized with epoxy groups [30]. The SSO was prepared by hydrolytic condensation of TOHES using DGEBA as a solvent. The reaction was catalyzed by formic acid keeping a H_2O/Si molar ratio equal to 3. Formic acid acts as a catalyst promoting the condensation through the formation of sililformates as intermediate species [33]. As hydrolytic condensation of TOHES takes place, higher molar mass molecules are generated. However, intramolecular condensation reactions also occur, leading to cage-like molecules with few or no reactive silanol groups. Therefore, the distribution of species in the final product is governed by a competition between inter- and intramolecular condensation reactions [30].

For reference, the SEC chromatograms of both TOHES and DGEBA are shown in Fig. 2. These are compounds of low molar mass (247 and 340 g/mol, respectively) and therefore have longer retention time in SEC (41.7 min), as shown in Fig. 2a and b. Fig. 2c shows the SEC chromatogram of the products obtained after the hydrolytic condensation of TOHES in the presence of DGEBA (SSO/DGEBA). The peak that appears at 40.5 min in Fig. 2c was assigned to species containing four Si atoms, based on polystyrene (PS) standards. The next peak appearing at 39.1 min had an average mass that was about twice the mass of the previous one, based on PS standards. It was thus assigned to clusters of perfect and imperfect polyhedra containing eight Si atoms. The broad peak centered at 36.1 min represents the envelope of a number of higher-molar-mass peaks corresponding to clusters of species with 16 and even more Si atoms, based on PS standards.

A further characterization of the species present in the SSO/DGEBA mixture was performed by UV-MALDI MS. Fig. 3a shows the full mass spectrum using GA as a matrix, whereas Fig. 3b is a magnification of the molar mass distribution in the *m/z* range from 400 to 2600. In every case, the cations correspond to particular species that added a Na^+ ion. It was observed a distribution of species peaking in the *m/z* range between 449.8 and 3986.4, which corresponds to species with 2–22 Si atoms, being the most abundant species the ones containing between 7 and 14 Si atoms. Every cluster in Fig. 3b contains several peaks assigned to species with the same number of Si atoms but different degrees of intramolecular condensation. As expected, the *m/z* difference between two consecutive peaks is equal to 18, corresponding to the release of one water molecule. Since the most intense peak of every cluster is at a high *m/z* value, we can infer that most of the species are incompletely condensed structures with a small fraction of perfect polyhedra.

Although Fig. 2c and Fig. 3 show the presence of high molar mass species, the stability of the synthesized SSO with respect to

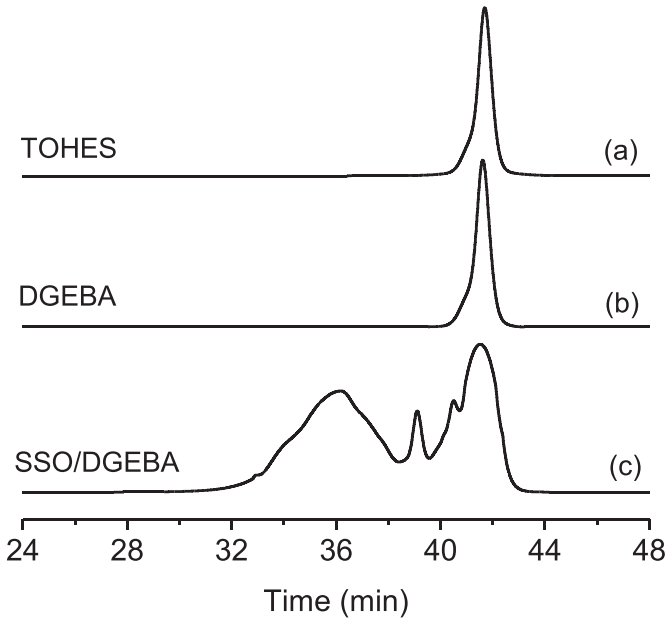

Fig. 2. SEC chromatograms of: (a) TOHES; (b) DGEBA; (c) products obtained from the hydrolytic condensation of TOHES in the presence of DGEBA as a solvent (30:70 SSO/DGEBA formulation).

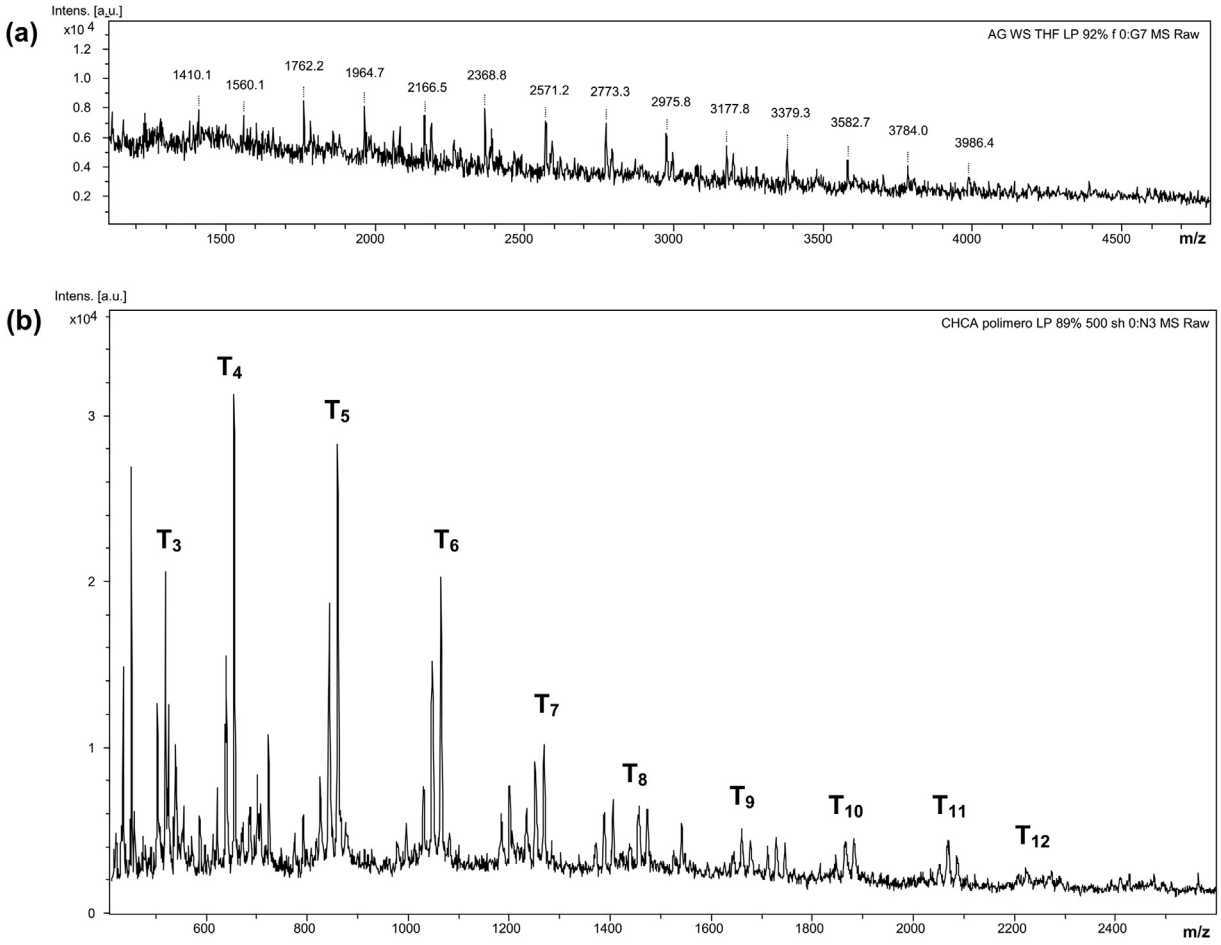

Fig. 3. UV-MALDI MS of the 30:70 SSO/DGEBA formulation (positive mode; matrix GA; sample doped with NaCl). (a) Full scale spectrum, and (b) magnification in the *m/z* range from 400 to 2600.

gelation or precipitation was excellent, even after several months of storage at 4 °C. FTIR analysis of a freshly synthesized 30:70 SSO/DGEBA sample exhibited a spectrum nearly identical to that of a sample stored at 4 °C and analyzed after 2 months (see Fig. S1 in Supplementary Material). This is an important aspect to consider for application purposes.

Using IR spectroscopy, we confirmed that the epoxy rings of both DGEBA and TOHES did not react during hydrolytic condensation, even after the thermal treatment at 140 °C (Fig. 4a and b). This was proved by the constancy of the ratio of heights of the absorption bands of the epoxy rings in DGEBA (4530 cm^{-1}) and in TOHES (884 cm^{-1}) with respect to the reference bands (4620 cm^{-1} and 1608 cm^{-1} for DGEBA and TOHES respectively).

3.2. Visible light photopolymerization

TOHES and DGEBA displayed different reactivity in photoinitiated cationic ring-opening polymerization, which can be readily ascertained by examining their conversion vs. time plots as determined by FTIR (Fig. 5). In both cases, the three-component initiator system (Ph_2ISbF_6, CQ and EDMAB) was used, and irradiations were conducted with a LED unit operating in the visible region of the spectrum (410–530 nm, 600 mW/cm^2). The possible initiating mechanism previously reported is briefly described here [14,16]. Irradiation with visible light produces the excitation of CQ to its singlet, which is rapidly converted to its triplet state by intersystem crossing. The excited CQ molecule is reduced by EDMAB, giving place to ketyl and α-amino free radicals. These radicals are oxidized by the diaryliodonium salt (Ph_2ISbF_6) to generate cationic species, which initiate the cationic ring-opening polymerization of epoxy monomers.

Fig. 5 shows that TOHES and DGEBA present two extreme behaviors under cationic ring-opening photopolymerization conditions at room temperature. TOHES underwent very rapid polymerization on visible light irradiation, resulting in a percent conversion of 99% after 10 s irradiation. In contrast, under the same conditions, DGEBA underwent very slow photopolymerization. In fact, no significant conversion of this monomer was detected after 40 s irradiation. The different responses of these two monomers can be related to their structures. Crivello and co-workers reported a detailed study on the reactivity of a wide variety of epoxy monomers, and concluded that the epoxide ring strain is one of the most important factors in determining their reactivity [17,34,35]. These authors found that monomers containing the highly strained epoxycyclohexane and epoxycyclopentane rings are considerably more reactive than open-chain epoxy compounds. In addition, glycidyl ether-type epoxide monomers (such as DGEBA) contain neighboring oxygen atoms in the molecule that are located such that they can stabilize the intermediate protonated species (oxonium ions), retarding the growth of the chain ends. These monomers underwent slow photoinitiated cationic polymerization at room temperature (Fig. 5).

Experiments were carried out to determine whether photopolymerization of DGEBA can be effectively accelerated by

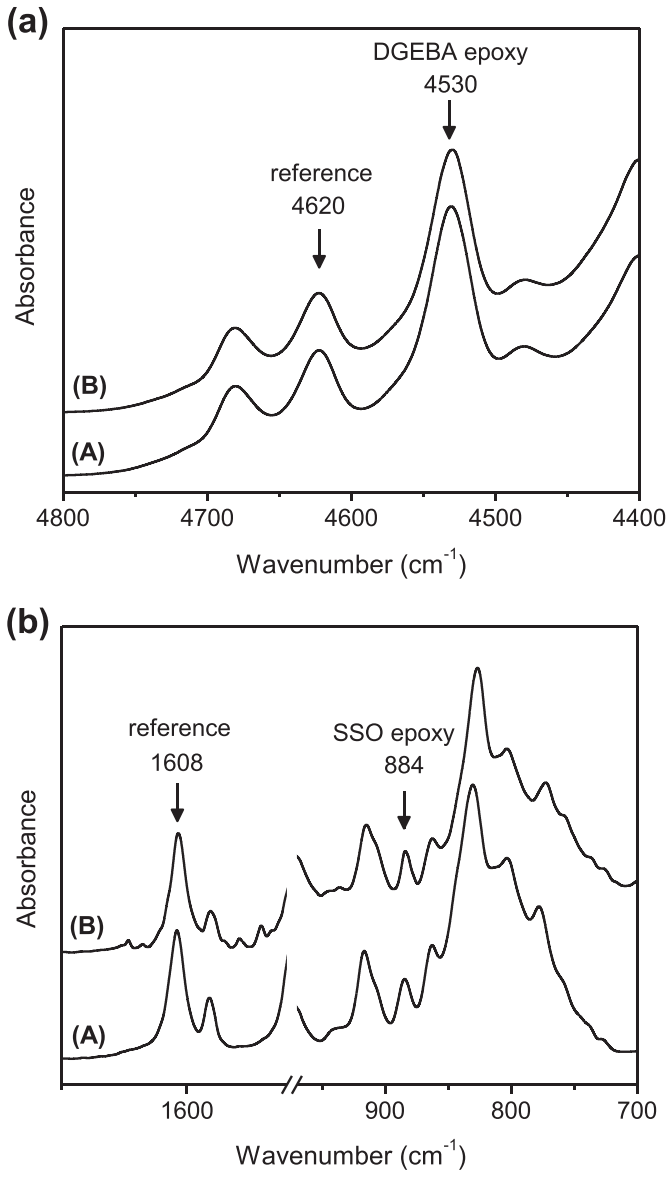

Fig. 4. FTIR spectra of: (trace A) 30:70 TOHES/DGEBA mixture before hydrolytic condensation; (trace B) 30:70 SSO/DGEBA mixture after hydrolytic condensation. (a) NIR; and (b) MIR.

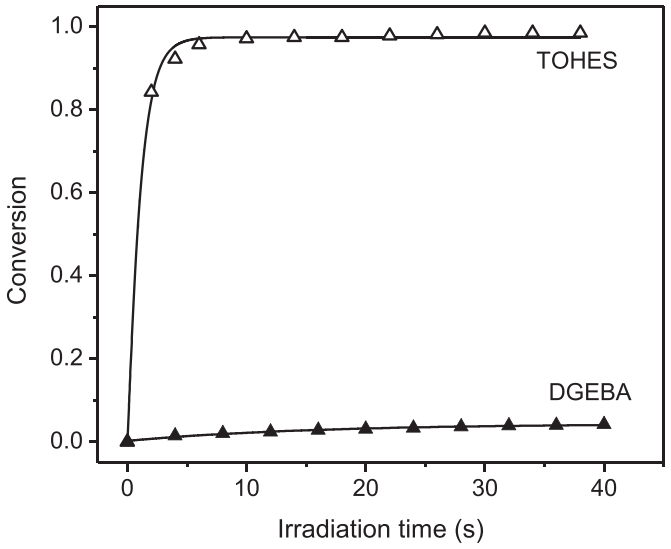

Fig. 5. Comparison of the behaviors of TOHES and DGEBA under cationic ring-opening photopolymerization conditions at room temperature. The monomers were photoactivated with 2 wt% Ph_2ISbF_6 in combination with 1wt% CQ and 1 wt% EDMAB. Irradiations were conducted with a LED unit operating in the visible region of the spectrum (410–530 nm, 600 mW/cm^2). Lines are drawn to guide the eye.

conducting the reaction in the presence of the SSO functionalized with highly reactive epoxycyclohexane groups. To explore this possibility, the SSO/DGEBA solution obtained after hydrolytic condensation of TOHES was diluted with appropriate amounts of DGEBA to prepare samples where the contribution of epoxy groups from the SSO varies between 30% and 10%. The photoactivated samples were irradiated for periods of 4 s and NIR spectra were collected immediately after each exposure interval. Fig. 6 shows the conversion of epoxy groups from DGEBA as a function of irradiation time for the tested samples. As may be noted, the polymerization of DGEBA was markedly accelerated as the amount of SSO in the reaction mixture was increased. For example, for 60 s of irradiation, the percent conversion of epoxy groups from DGEBA increased from 4% in neat DGEBA to 37% and 51% in the 20:80 and 30:70 SSO/DGEBA blends respectively. We interpret that the polymerization of DGEBA is accelerated by copolymerization effects with the more reactive epoxy groups from the SSO. Thus, the polymerization rate of DGEBA increases with the content of SSO as the number of highly reactive oxonium intermediates formed by the SSO increases.

To understand whether the structure of the SSO has any effect on the activation of DGEBA polymerization, we tested a 20:80 blend where the SSO was replaced by a commercial biscycloaliphatic epoxy monomer (3,4-epoxycyclohexylmethyl 3,4-epoxycyclohexanecarboxylate (EEC)). The conversion vs. irradiation time curves for the 20:80 SSO/DGEBA and 20:80 EEC/DGEBA blends are shown in Fig. 7a and b respectively. To aid in the comparison of these results, we plotted the conversion of DGEBA vs. conversion of cycloaliphatic epoxy groups for both blends (Fig. 7c). It can be seen that both SSO and EEC activate DGEBA polymerization, although SSO makes it to a greater extent than EEC. These results suggest the diffusional and topological constraints due to the polyhedral structure of the SSO make the oxonium cations formed by the SSO react with DGEBA to a greater extent than the oxonium cations formed by EEC.

Previously [36], we have reported that a neat DGEBA sample photopolymerized under visible light irradiation (at 60 mW/cm^2, in the 390–800 nm range) at room temperature reached a conversion of 46% after 24 h irradiation. We also demonstrated that, at room temperature, neat DGEBA reaches the glassy state at that conversion level. As shown in Fig. 6, only a few seconds of irradiation (at 600 mW/cm^2, in the 410–530 nm range) are enough for the onset of vitrification in the 30:70 SSO/DGEBA formulation.

Better results were obtained under continuous irradiation conditions. Table 1 displays the conversion of epoxy groups from DGEBA and SSO, as well as the overall conversion of epoxy groups, in SSO/DGEBA blends photopolymerized under continuous irradiation. As can be noted, a sample irradiated for 60 s under continuous mode reached higher conversion of the epoxy groups from DGEBA than the same sample irradiated for periods of 4 s during a total time of 60 s (Fig. 6). The same feature was observed for all the formulations tested.

These results cannot be ascribed as due solely to the copolymerization of DGEBA with the more reactive epoxy groups from the SSO. Evidently, thermal effects must contribute to these results. The polymerization reaction is highly exothermic, which results in an

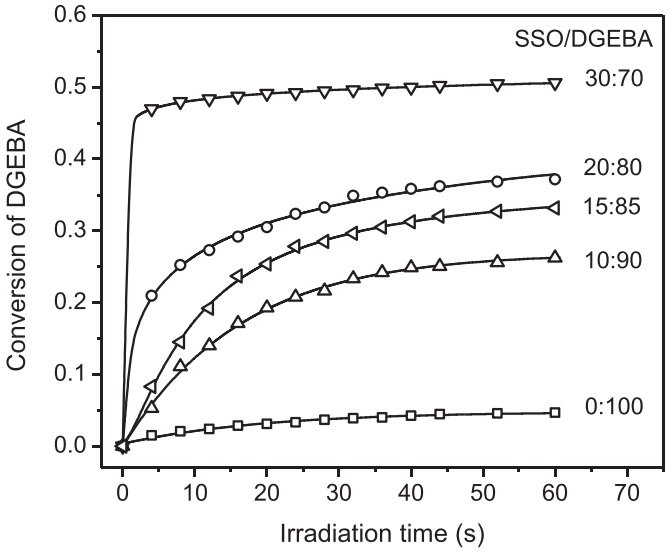

Fig. 6. Conversion of epoxy groups from DGEBA in SSO/DGEBA blends versus irradiation time. The blends were photoactivated with 2 wt% Ph_2ISbF_6 in combination with 1wt% CQ and 1 wt% EDMAB. Irradiations were conducted with a LED unit operating in the visible region of the spectrum (410–530 nm, 600 mW/cm^2). Lines are drawn to guide the eye.

3.3. Temperature evolution during photopolymerization

To quantify the thermal effects produced in the course of photopolymerization, the temperature of the sample was monitored as a function of the continuous irradiation time. As a control test, we first measured a non-initiated DGEBA sample. Only a very small temperature increase (between 3 and 4 °C over 3 min of irradiation) was observed when the sample was irradiated in the absence of photoinitiator (see Fig. S2 in Supplementary Material). Therefore, we can rule out the visible light irradiation as a considerable source of heat.

No significant change in temperature was recorded during irradiation of a photoactivated sample of neat DGEBA (Fig. 8a). However, it can be seen that the temperature of the samples containing SSO rapidly increased with the irradiation time as a result of the most rapid rate of polymerization. As may be noted, the 10:90 SSO/DGEBA sample attained a maximum temperature of 74 °C at 64 s irradiation. When compared with this sample, the 15:85 blend experienced an appreciable increase in the polymerization rate, together with a marked rise of the maximum temperature attained (higher than 105 °C). This is consistent with the higher content of epoxy groups provided by the SSO in this last formulation. However, to our surprise, we found that when further increasing the amount of SSO in the blend, the maximum temperature progressively decreased. To highlight this effect, we plotted the ultimate temperature attained during the photopolymerization as a function of the number of epoxy groups provided by the SSO (Fig. 8b). It can be seen that the maximum temperature first increased with the addition of SSO, reached a maximum at 15%, and then gradually decreased.

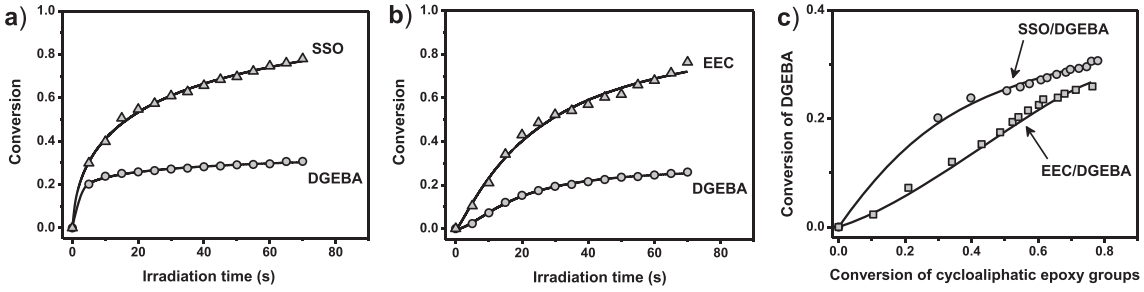

Fig. 7. (a) Conversion of epoxy groups from DGEBA and SSO versus irradiation time in the 20:80 SSO/DGEBA blend. (b) Conversion of epoxy groups from DGEBA and EEC versus irradiation time in the 20:80 EEC/DGEBA blend. (c) Conversion of DGEBA versus conversion of cycloaliphatic epoxy groups in the 20:80 SSO/DGEBA and 20:80 EEC/DGEBA blends. The blends were photoactivated with 2 wt% Ph_2ISbF_6 in combination with 1wt% CQ and 1 wt% EDMAB. Irradiations were conducted with a LED unit operating in the visible region of the spectrum (410–530 nm, 600 mW/cm^2). Lines are drawn to guide the eye.

Table 1
Conversion of epoxy groups from DGEBA and SSO, and overall conversion percentage of epoxy groups in SSO/DGEBA blends irradiated for 60 s under continuous irradiation (410–530 nm, 600 mW/cm^2).

Sample	% Conversion of DGEBA	% Conversion of SSO	% Overall conversion of epoxy groups
0:100 SSO/DGEBA	5.4 (±0.3)	- -	5.4 (±0.3)
10:90 SSO/DGEBA	41.4 (±2.7)	89.0 (±5.6)	46.2 (±2.9)
15:85 SSO/DGEBA	46.8 (±1.6)	81.1 (±2.8)	51.9 (±1.8)
20:80 SSO/DGEBA	59.7 (±1.5)	71.7 (±1.9)	62.1 (±1.6)
30:70 SSO/DGEBA	60.2 (±1.9)	69.1 (±3.1)	62.8 (±2.1)

increase in the sample temperature during the process [17]. In the first mode (Fig. 6), samples were irradiated for a short time and then, during collection of the NIR spectrum, heat was dissipated and the sample temperature fell rapidly. In contrast, continuous irradiation led to excessive heat build-up, which resulted in a substantial increase in the sample temperature. A higher sample temperature induced an increase in the mobility of the reaction environment (i.e. monomers, oxonium ion intermediates and polymer) and consequently increased both the reaction rate and the vitrification conversion. The temperature evolution during polymerization will be examined in more detail in the next section.

To aid in the interpretation of these results, we evaluated the heat capacity at constant pressure (*Cp*) of the different SSO/DGEBA formulations. For these tests, we first measured a DSC curve in dynamic mode for each sample and then computed its *Cp* value by applying eqn. (1) in the manner described in the Experimental

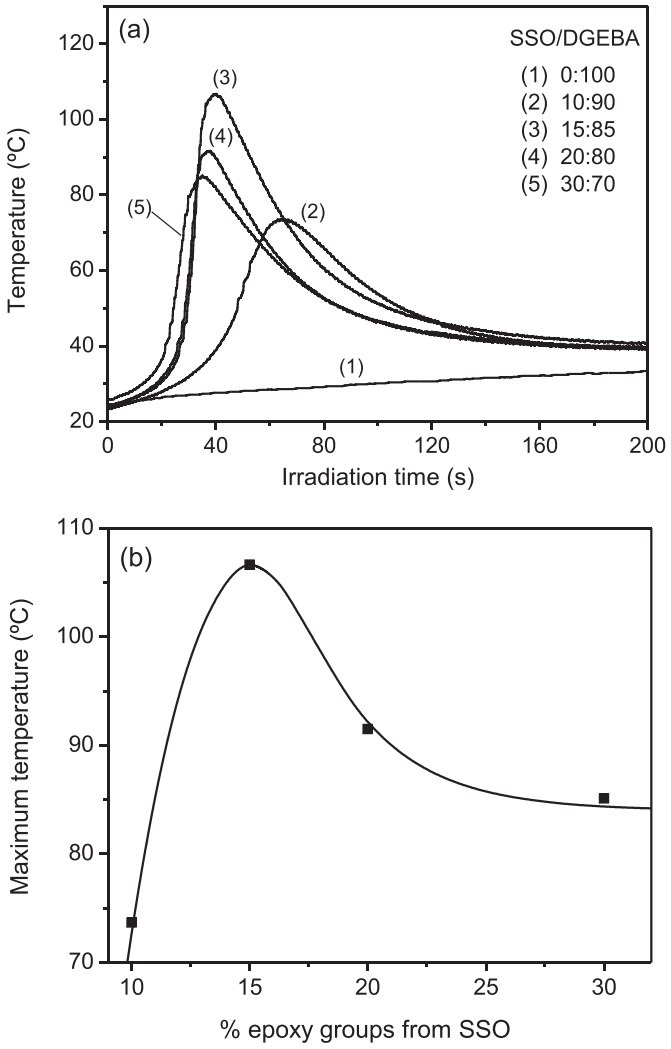

Fig. 8. Thermal effects produced in the course of the photopolymerization of SSO/DGEBA blends. The blends were photoactivated with 2 wt% Ph_2ISbF_6 in combination with 1wt% CQ and 1 wt% EDMAB. Irradiations were conducted with a LED unit operating in the visible region of the spectrum (410–530 nm, 600 mW/cm^2). (a) Temperature evolution during continuous irradiation time. (b) Maximum temperature attained during photopolymerization as a function of the percentage of epoxy groups provided by the SSO. The line is drawn to guide the eye.

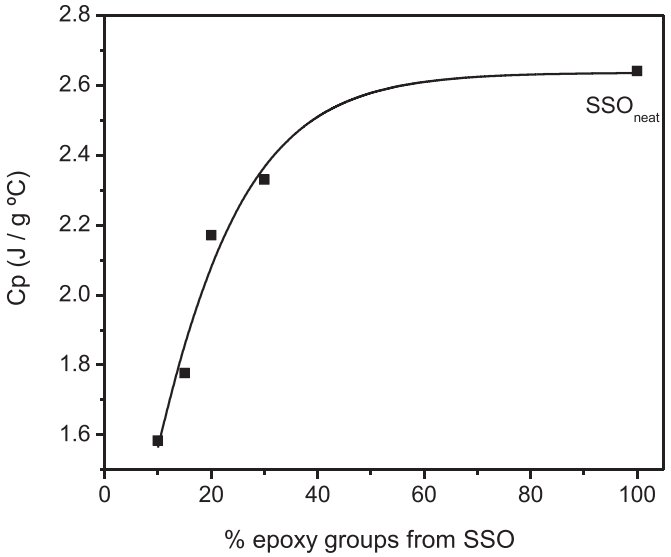

Fig. 9. Heat capacity at constant pressure (*Cp*) of SSO/DGEBA blends as a function of the percentage of epoxy groups provided by the SSO. The line is drawn to guide the eye.

Section. The *Cp* value of a SSO synthesized in the absence of DGEBA (denoted SSO_{neat}) was also assessed. Fig. 9 shows the *Cp* of the mixture as a function of the number of epoxy groups provided by the SSO. As can be seen, as the SSO content increased, the *Cp* of the mixture increased significantly. As a first approximation, we can consider that in the short period of time in which the temperature rises during irradiation (see Fig. 8a) the system has a pseudo-adiabatic behavior. Under this assumption, we can explain the trend shown in Fig. 8b as the result of a competition between two effects. With increasing SSO content, more heat is produced due to the highly exothermic polymerization, but also, more heat is required by the system to increase its temperature. The competition between these two effects would explain the maximum observed in Fig. 8b. The 10:90 SSO/DGEBA sample was excluded from this analysis because its temperature rise was slow and thus the heat generated by polymerization was partially dissipated.

Based on these results, we suggest that DGEBA may undergo rapid photopolymerization in the presence of SSO due to a combination of thermal effects (due to the heat released by ring-opening polymerization) and copolymerization effects. It is worth noting that while the maximum temperature attained by the 15:85 sample was the highest of all the formulations studied, this sample achieved a lower final epoxy conversion (51.9 ± 1.8) than the 20:80 and 30:70 samples (62.1 ± 1.6 and 62.8 ± 2.1 respectively). This is because with increasing SSO content, the T_g shifted to lower temperatures, as discussed in the next section.

3.4. Thermomechanical properties of the resulting networks

The network properties of the resulting light-cured samples were investigated by dynamic mechanical analysis (DMA). For comparison purposes, we also tested a set of samples subjected to a thermal postcuring treatment (at 180 °C for 2 h) after photo-irradiation. We found that after the thermal treatment, the overall conversion of epoxy groups advanced to around 90% for all the SSO/DGEBA samples tested. The postcuring effect is assumed to be due to the activation of the reactive species that remained alive when the sample was devitrified. Evidently, the maximum conversions in these highly crosslinked matrices approach, but do not reach, 100% due to the limited mobility and restricted diffusion in these systems.

The photo-irradiation of all the SSO/DGEBA formulations studied during the course of this work leads to transparent, glassy and completely tack-free materials. The transmittance spectrum of the photo-cured 30:70 SSO/DGEBA hybrid material is shown in the Supplementary Material (Fig. S4). SEM photographs of the photo-cured materials showed flat fracture surfaces with no phase-separation features, and this was in agreement with the transparency of these samples (see Fig. S5 in the Supplementary Material). Table 2 summarizes the DMA results in terms of storage modulus (E') for the materials obtained after irradiation and the materials subjected to the additional thermal postcuring treatment. As a control epoxy network, we used a neat DGEBA sample fully cured by thermal cationic polymerization with $BF_3 \cdot MEA$ as initiator (details regarding the preparation protocol are shown in the Supplementary Material). The data in Table 2 show that after irradiation, the SSO/DGEBA formulations studied produced networks with E' values in the glassy region (evaluated at $T = 30$ °C) as high as the control DGEBA network. Furthermore, no significant differences in

Table 2
Storage modulus (E') at 30 °C and at 50 °C above T_g for the materials obtained after irradiation and the materials subjected to an additional thermal postcuring treatment.

Sample	After irradiation[a]	After thermal postcuring[b]	
	E' at 30 °C (GPa)	E' at 30 °C (GPa)	E' at 50 °C above T_g (MPa)
Neat DGEBA (control)[c]	- -	1.09 (±0.03)	44.2 (±1.2)
10:90 SSO/DGEBA	1.08 (±0.04)	0.95 (±0.09)	46.6 (±0.7)
15:85 SSO/DGEBA	1.07 (±0.09)	1.11 (±0.05)	47.9 (±3.0)
20:80 SSO/DGEBA	1.09 (±0.10)	1.01 (±0.08)	50.8 (±5.1)
30:70 SSO/DGEBA	1.04 (±0.11)	1.02 (±0.03)	85.9 (±3.8)

[a] Continuous irradiation for 120 s on each side of the specimen (410–530 nm, 600 mW/cm^2).
[b] Heating at 180 °C for 2 h.
[c] The neat epoxy network was obtained using BF_3·MEA as initiator. Curing was carried out at 140 °C for 3 h, and postcuring at 180 °C for 2 h.

the values of E' at 30 °C were observed after subjecting these irradiated materials to an additional postcuring treatment (see Table 2). This is because in the glassy state the modulus is mainly dependent on the interaction between chains rather than on the degree of crosslinking and conversion [37].

The DMA spectra in terms of E' and loss factor (tan δ) for the materials subjected to the additional thermal postcuring treatment are shown in Fig. 10a and b respectively. It can be seen that the E' values in the rubbery state increased as the SSO content in the formulation increased. For reference, the E' values taken at 50 °C above the glass transition temperature are listed in Table 2. As the rubbery modulus is proportional to the crosslink density, we can conclude that the SSO species function as multifunctional epoxy reactants with average epoxy functionality greater than that of DGEBA.

All tan δ profiles (Fig. 10b) showed the occurrence of one α-relaxation (corresponding to T_g), indicating single-phase network structure. This is expected, since, as already mentioned, all the samples were found homogeneous and visually transparent after photo-irradiation and postcuring treatment. This is additional evidence that copolymerization between DGEBA and SSO occurs during network formation. With increasing SSO content, the α-relaxation shifted to lower temperatures from 166 °C for the control neat DGEBA to 146 °C and 135 °C in the 20:80 and 30:70 SSO/DGEBA samples respectively. As discussed above, the addition of SSO increased the concentration of crosslink points in the network and this should in principle shift the α-relaxation to higher temperatures. However, the presence of SSO commonly increases both the amount of free-volume and the average flexibility of chains in the epoxy network, and these effects act in the opposite sense, i.e., shift the α-relaxation towards lower temperatures [25,38]. Based on these arguments, we suggest that the prevailing trend should be attributed to free-volume effects and enhanced chain mobility produced by the presence of SSO in the epoxy network.

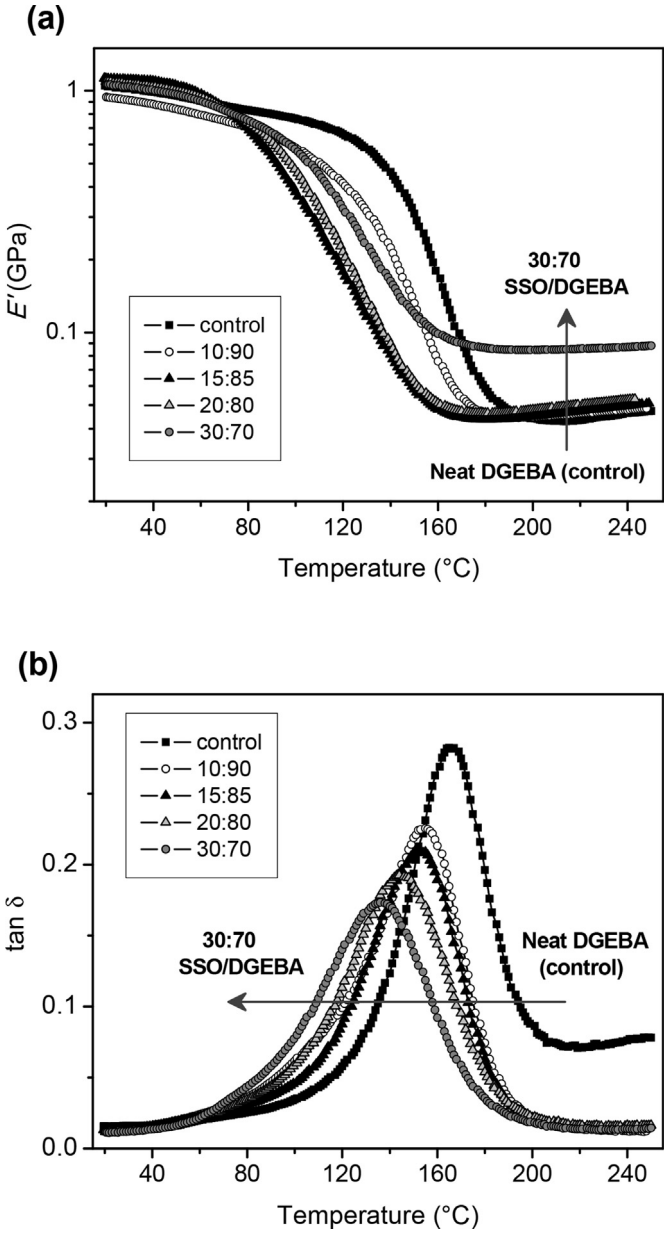

Fig. 10. Dynamic mechanical analysis data for the materials subjected to a thermal postcuring treatment after photo-irradiation: (a) storage modulus (E') and (b) loss factor (tan δ).

4. Conclusions

In this report, we showed that the slow cationic ring-opening photopolymerization of aryl glycidyl ether monomers, such as DGEBA, can be markedly accelerated by combining them with SSO functionalized with reactive epoxycyclohexane groups. The SSO was prepared by hydrolytic condensation of TOHES using DGEBA as a solvent. The epoxy functional groups remained unreacted during the hydrolytic condensation process as revealed by FTIR spectroscopy. The resulting SSO showed very good stability with respect to gelation or precipitation, even after several months of storage at 4 °C. The photopolymerization of DGEBA was markedly accelerated as the amount of SSO increased. The promoter effect on the reactivity of DGEBA was ascribed to a combination of thermal effects (due to the heat released by ring-opening polymerization) and copolymerization effects. The resulting light-cured materials exhibited good mechanical characteristics at room temperature, similar to those of a neat epoxy network fully cured by thermal

cationic polymerization. Using dynamic mechanical analysis, we demonstrated that the resulting hybrid materials present a single-phase network structure, where the SSO species function as highly multifunctional epoxy reactants. The approach delivered in this study can offer the possibility of greatly increasing the use of aryl glycidyl ether monomers in a variety of high speed photocuring applications.

Acknowledgments

The financial support of the following institutions is gratefully acknowledged: National Research Council (CONICET, Argentina), National Agency for the Promotion of Science and Technology (ANPCyT, Argentina), andUniversity of Mar del Plata.

Appendix A. Supplementary data

Supplementary data related to this article can be found at http://dx.doi.org/10.1016/j.polymer.2015.12.013.

References

[1] (a) J.V. Crivello, in: D.J. Brunelle (Ed.), Ring Opening Polymerization, Hanser, Munich, 1993, p. 157;
(b) J.V. Crivello, in: N.S. Allen (Ed.), Development in Polymer Photochemistry 2, Applied Sciences, London, 1981, pp. 1–38.
[2] M. Jang, J.V. Crivello, J. Polym. Sci. Part A Polym. Chem. 41 (2003) 3056–3073.
[3] Y. Yagci, S. Jockusch, N.J. Turro, Macromolecules 43 (2010) 6245–6260.
[4] J.P. Fouassier, Photoinitiation, Photopolymerization, and Photocuring: Fundaments and Applications, Hanser/Gardner publications, Munich, 1995.
[5] Y. Yagci, Macromol. Symp. 240 (2006) 93–101.
[6] J.V. Crivello, J. Macrom. Sci. Pure Appl. Chem. 46 (2009) 474–483.
[7] M. Sangermano, G. Malucelli, R. Bongiovanni, A. Priola, U. Annby, N. Rehnberg, Eur. Polym. J. 38 (2002) 655–659.
[8] J.P. Pascault, R.J.J. Williams, General concepts about epoxy polymers, in: J.P. Pascault, R.J.J. Williams (Eds.), Epoxy Polymers, Wiley-VCH, Weinheim, 2010, pp. 1–5.
[9] J.V. Crivello, J.H.W. Lam, Macromolecules 10 (1977) 1307–1315.
[10] J.V. Crivello, J.H.W. Lam, J. Polym. Sci. Part A Polym. Chem. 16 (1978) 2441–2451.
[11] J.V. Crivello, J.H.W. Lam, J. Polym. Sci. Part A Polym. Chem. 17 (1979) 977–999.
[12] J.V. Crivello, Y. Hua, Z. Gomurashvili, Macromol. Chem. Phys. 202 (2001) 2133–2141.
[13] Z. Gomurashvili, J.V. Crivello, J. Polym. Sci. Part A Polym. Chem. 39 (2001) 1187–1197.
[14] J.V. Crivello, M. Sangermano, J. Polym. Sci. Part A Polym. Chem. 39 (2001) 343–356.
[15] J.V. Crivello, J. Polym. Sci. Part A Polym. Chem. 47 (2009) 866–875.
[16] W.F. Schroeder, S.V. Asmussen, M. Sangermano, C.I. Vallo, Polym. Int. 62 (2013) 1368–1376.
[17] U. Bulut, J.V. Crivello, Macromolecules 38 (2005) 3584–3595.
[18] S.C. Lapin, Radiation curing of polymeric materials, in: C.E. Hoyle, J.F. Kinstle (Eds.), ACS Symposium Series No. 417, American Chemical Society, Washington, DC, 1990, pp. 361–381.
[19] S. Penczek, P. Kubisa, K. Matyjaszewski, Cationic ring-opening polymerization of heterocyclic monomers, in: Advances in Polymer Science vol. 37, Springer-Verlag, Berlin, 1980, pp. 1–2.
[20] J.V. Crivello, J.H.W. Lam, J.E. Moore, S.H. Schroeter, J. Radiat. Curing 5 (1978) 2–17.
[21] K.J. Ivin, T. Saegusa, Ring-opening Polymerization, Elsevier Applied Science Publishers, New York, 1984, p. 28.
[22] R.H. Baney, M. Itoh, A. Sakakibara, T. Suzuki, Chem. Rev. 95 (1995) 1409–1430.
[23] J. Choi, R. Tamaki, S.G. Kim, R.M. Laine, Chem. Mater. 15 (2003) 3365–3375.
[24] P.T. Mather, H.G. Jeon, A. Romo-Uribe, T.S. Haddad, J.D. Lichtenhan, Macromolecules 32 (1999) 1194–1203.
[25] I.E. dell'Erba, R.J.J. Williams, Eur. Polym. J. 43 (2007) 2759–2767.
[26] I.E. dell'Erba, D.P. Fasce, R.J.J. Williams, R. Erra-Balsells, Y. Fukuyama, H. Nonami, Macromol. Mater. Eng. 289 (2004) 315–323.
[27] K.M. Schreck, D. Leung, C.N. Bowman, Macromolecules 44 (2011) 7520–7529.
[28] L. Matëjka, POSS and other hybrid epoxy polymers, in: J.P. Pascault, R.J.J. Williams (Eds.), Epoxy Polymers, Wiley-VCH, Weinheim, 2010, pp. 137–157.
[29] K. Pielichowski, J. Njuguna, B. Janowski, J. Pielichowski, Adv. Polym. Sci. 201 (2006) 225–296.
[30] P. Eisenberg, R. Erra-Balsells, Y. Ishikawa, J.C. Lucas, A.N. Mauri, H. Nonami, C.C. Riccardi, R.J.J. Williams, Macromolecules 33 (2000) 1940–1947.
[31] E. Morîntale, A. Harabor, C. Constantinescu, P. Rotaru, Phys. AUC 23 (2013) 89–94.
[32] H. Nonami, S. Fukui, R. Erra-Balsells, J. Mass. Sectrom. 32 (1997) 287–296.
[33] K. Sharp, J. Sol-Gel Sci. Technol. 2 (1994) 35–41.
[34] J.V. Crivello, U. Varlemann, J. Polym. Sci. Part A Polym. Chem. 33 (1995) 2473–2486.
[35] M. Jang, J.V. Crivello, J. Polym. Sci. Part A Polym. Chem. 41 (2003) 3056–3073.
[36] I.A. Zucchi, W.F. Schroeder, Polymer 56 (2015) 300–308.
[37] J.P. Pascault, H. Sautereau, J. Verdu, R.J.J. Williams, Thermosetting Polymers, Marcel Dekker, New York, 2002, pp. 323–348.
[38] G. Ragosta, P. Musto, M. Abbate, G. Scarinzi, Polymer 50 (2009) 5518–5532.